Environmental Science & Technology

Article

pubs.acs.org/est

Load-Dependent Emission Factors and Chemical Characteristics of IVOCs from a Medium-Duty Diesel Engine

Eben S. Cross,*[,†,∥] Alexander G. Sappok,[‡,⊥] Victor W. Wong,[‡] and Jesse H. Kroll[†,§]

[†]Department of Civil and Environmental Engineering, [‡]Sloan Automotive Laboratory, and [§]Department of Chemical Engineering, Massachusetts Institute of Technology, Cambridge, Massachusetts, 02139 United States

[∥]Aerodyne Research Inc., Billerica, Massachusetts, 01821 United States

[⊥]Filter Sensing Technologies Inc., Malden, Massachusetts, 02148 United States

Supporting Information

ABSTRACT: A detailed understanding of the climate and air quality impacts of mobile-source emissions requires the characterization of intermediate-volatility organic compounds (IVOCs), relatively-low-vapor-pressure gas-phase species that may generate secondary organic aerosol with high yields. Due to challenges associated with IVOC detection and quantification, IVOC emissions remain poorly understood at present. Here, we describe measurements of the magnitude and composition of IVOC emissions from a medium-duty diesel engine. Measurements are made on an engine dynamometer and utilize a new mass-spectrometric instrument to characterize the load dependence of the emissions in near-real-time. Results from steady-state engine operation indicate that IVOC emissions are highly dependent on engine power, with highest emissions at engine idle and low-load operation (≤25% maximum rated power) with a chemical composition dominated by saturated hydrocarbon species. Results suggest that unburned fuel components are the dominant IVOCs emitted at low loads. As engine load increases, IVOC emissions decline rapidly and become increasingly characterized by unsaturated hydrocarbons and oxygenated organics, newly formed from incomplete combustion processes at elevated engine temperatures and pressures. Engine transients, including a cold-start ignition and engine acceleration, show IVOC emission profiles that are different in amount or composition compared to steady-state combustion, underscoring the utility of characterizing IVOC emissions with high time resolution across realistic engine operating conditions. We find possible evidence for IVOC losses on unheated dilution and sampling surfaces, which need to be carefully accounted for in IVOC emission studies.

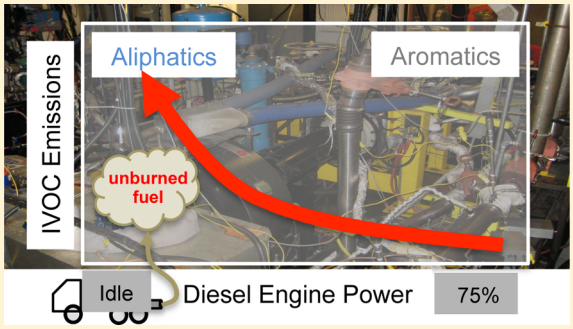

INTRODUCTION

Emissions of organic species from mobile sources include air toxics, primary organic aerosol (POA), and precursors of ozone and secondary organic aerosol (SOA) and hence have important impacts on air quality,[1,2] climate, and human health.[3−5] Measurements of organic species from engines have traditionally focused on emissions of volatile organic compounds (VOCs)[6] and POA,[7,8] which are directly related to regulations targeting ozone and primary particles. However, recent work has demonstrated the potential importance of an additional class of compounds, intermediate-volatility organic compounds (IVOCs), gas-phase species with effective saturation concentrations (c^*) between 10^3 and 10^6 $\mu g\ m^{-3}$. Such species have been shown to serve as important precursors to SOA[9,10] and thus are likely to play a major role in the air quality and climate impacts of mobile sources.[6,11,12]

While total hydrocarbon emissions from mobile sources have been shown to depend on engine design, operation, and fuel formulation[13,14] at present, relatively little is known about the amounts and chemical composition of combustion-related IVOCs. This arises largely from the lack of analytical methods that can accurately measure and quantify IVOCs with high temporal resolution, as well as the extreme chemical complexity of IVOC mixtures. Previous measurements of IVOCs from mobile sources have utilized offline chromatographic techniques for IVOC quantification and speciation[15−17] or used the differences between concentrations of VOCs and total nonmethane organic gases (NMOG) to infer IVOC emissions.[6,18] Studies of IVOCs from diesel engines, the focus of the present work, have demonstrated that IVOCs comprise a significant fraction (~20−60%) of NMOG emissions.[15−18] Measurements of the chemical composition of the emitted IVOCs showed some similarities to unburned diesel fuel.[15] However, only a small fraction (10−20%) of the total IVOC mass is routinely speciated, with the remainder characterized as "unresolved complex mixture" (UCM), likely made up of cyclic and branched hydrocarbon species.[15−17]

Received: August 17, 2015
Revised: October 8, 2015
Accepted: October 13, 2015
Published: October 13, 2015

DOI: 10.1021/acs.est.5b03954
Environ. Sci. Technol. 2015, 49, 13483−13491

These previous studies of diesel IVOC emissions were carried out using chassis dynamometers, with results averaged over an entire drive cycle. While this approach simulates real-world driving patterns and provides a benchmark for emissions comparisons between vehicles, it offers limited assessment of the combustion processes or specific engine operating conditions that control IVOC emissions.

IVOC emissions in diesel engines with no emissions control, such as the one used in this study, are clearly higher than diesels equipped with modern emission control technology (ECT).[17,18] While the fraction of non-ECT diesel engines in the United States and Europe is decreasing through recent regulations of on and off-road diesel systems, full adoption of ECTs is expected to be somewhat gradual due to the relatively long lifetime of diesel engines. As a result, non-ECT diesel engines may remain important sources of emissions in the United States and Europe over the coming decade. Engines with faulty, early generation, or tampered-with ECT systems may lead to emission profiles that more closely resemble non-ECT diesels. Moreover, the use of non-ECT diesel engines is widespread (and growing) throughout the developing world. Thus, unregulated (non-ECT) diesel emissions are expected to be an important and potentially dominant component of mobile-source emissions through 2040, especially in highly populated urban centers of the non-OECD economies.[19] There is, thus, a major need to understand the amounts and composition (and ultimately the atmospheric fate) of IVOC emissions from diesel combustion.

More generally, the magnitude and composition of IVOC emissions from diesel combustion (in ECT and non-ECT engines) are not well-constrained at present. Little is known about how they are affected by engine operation (engine power, speed, etc.), and even the source of IVOC emissions (unburned fuel, incomplete combustion products, products of the pyrolysis of fuel/lubricant, etc.) remains poorly understood. In recent years, uncertainties in IVOC amounts and chemistry have led to contrasting conclusions surrounding the relative impact of gasoline versus diesel combustion on regional air quality,[20−23] further motivating the development and application of improved IVOC characterization techniques. With this knowledge gap in mind, the aim of the current work is to better understand the factors and source processes that affect diesel IVOC emissions. We use a new near real-time mass spectrometric technique for characterizing the ensemble composition and amount of the IVOC emissions from a non-ECT medium duty diesel engine (MDDV) as a function of engine load. The high time resolution of the analytical technique also enables measurements of IVOC emissions during two engine "transients", a cold start and an acceleration from idle to low-load conditions, engine operating conditions that may produce disproportionately high IVOC emissions in both non-ECT and ECT-equipped diesel engines.[17]

EXPERIMENTAL SECTION

Engine and Emissions Sampling System. This study focuses on emissions from a Cummins preproduction development medium-duty diesel engine based on the 2002 ISB (Interact System B) 300 platform; as noted above, no ECT is used on this engine. The engine and emissions sampling system, located at MIT's Sloan Automotive Laboratory, have been described in detail in previous publications (specifications are given in Table S1).[24−26] All experiments utilized commercially available ultralow sulfur diesel fuel (ULSD, 15 ppm of S), and SAE 15W-40 CJ-4 diesel engine oil as lubricant; while emissions are likely to depend somewhat on the exact fuel and lubricant used, the investigation of such dependences is beyond the scope of this study.

An engine dynamometer was used to systematically vary the engine speed (∼700−2400 rpm; idle −75% max) and load (0−700 N m; idle −75% max). The present study focuses on a single engine load sweep, consisting of a cold-start ignition (with all components initially at ∼25 °C), a period of engine idle (0% load, with enough time for the engine and sampling system to reach thermal equilibrium), a stepwise upward ramp in engine load to 75% load, and a stepwise downward ramp back to engine idle.

Exhaust emissions were sampled from an unheated dilution tunnel built and designed specifically for emissions characterization.[27] A schematic of the experimental setup is provided in Figure S1. Briefly, engine exhaust is subsampled into the dilution tunnel from which IVOC emissions are sampled and characterized. The primary dilution ratio (which ranged from 2 to 6) was determined by monitoring the concentrations of CO_2 at two positions, the exit of the engine manifold (using nondispersive infrared spectroscopy, CAI 602P) and at the IVOC sampling point (using Fourier-transform infrared spectroscopy, MKS 2030). Sampling into the IVOC instrument (described below) was through a heated inlet system consisting of a 3.5 m length of 1/4 in. outer diameter stainless-steel tubing, coated with SilcoNert 2000 (Silcotek, Inc.) and held at 250 °C to reduce condensational losses. This inlet was located ∼2 m from the primary exhaust flow split, with the tip positioned at the center line of the 6 in. outer diameter dilution tunnel, oriented perpendicular to the flow. Sampled air passed through a SilcoNert-coated (SilcoTek, Inc.), heated metal filter to prevent refractory soot particles from clogging the capillary transfer lines of the instrument. The sampling flow rate through the IVOC inlet was held at 1.2 L min^{-1}, using a small diaphragm pump (UN86KTP KNF Neuberger, Inc.) to draw sample flow through the collector.

IVOC Measurements. The Thermal−Desorption Electron Ionization Mass Spectrometer (TD-EIMS) has been described previously;[28] only a brief overview is provided here to highlight the specific sampling and analysis procedures used in the current study. The instrument involves the cryogenic collection of sampled gases, followed by temperature-controlled desorption of the collected organics into the electron ionization region of a high-resolution time-of-flight mass spectrometer (TOF-WERK). In the current experiment, engine exhaust IVOCs were collected at −6° ± 2 °C for 60 s and desorbed from −6 to 280 °C over a period of 300 s, capturing an estimated volatility (c^*) range between 10^3 and 10^7 $\mu g\ m^{-3}$. The temperature was then held at 280 °C for an additional 60 s prior to cooling the system back to −6 °C via a flow of liquid N_2. Cooling times in this experiment were typically 90 s, allowing for IVOC measurements to be made every ∼8 min. During the temperature desorption ramp, "V-mode" high-resolution mass spectra were acquired at a rate of 1 Hz, allowing for the straightforward alignment of IVOC mass spectra with desorption temperature. Under these operating conditions, the mass resolving power of the instrument was ∼2000, providing unambiguous identification of major ions in the mass spectrum and clear separation of any $C_xH_y^+$ and $C_xH_yO_z^+$ ions at nominal masses below m/z 150. All identified carbon-containing ions, with the exception of CO^+ and CO_2^+, which had high background signals, were included in the analysis of

DOI: 10.1021/acs.est.5b03954
Environ. Sci. Technol. 2015, 49, 13483−13491

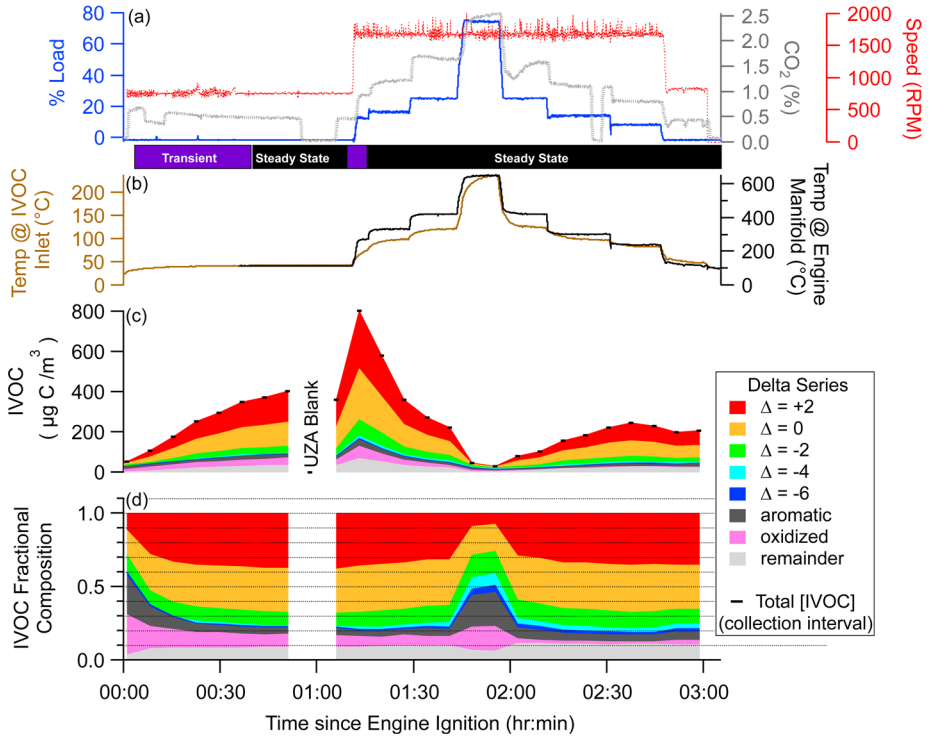

Figure 1. Summary of experimental parameters and measured IVOC emissions during a cold-start−load-sweep test cycle. Panels a and b show engine operating conditions (load, speed, and CO_2 concentrations), exhaust gas temperatures, and transient or steady-state sampling intervals. Panels c and d display the mass concentration and fractional composition (as Δ series contributions) of IVOC emissions. TD-EIMS collection intervals are indicated by the horizontal dashes displayed in panel c.

the mass spectrometric data. Estimates of H:C and O:C ratios are obtained from the high-resolution mass spectra using the approach of Aiken et al.,[29,30] though without any empirical correction accounting for effects of EI fragmentation. Such approximations may influence the absolute elemental ratios, but the qualitative differences in H:C and O:C at different engine operating conditions will not be affected.

Substantial organic signal was measured even when the engine was off. At times during the experiment, ultrazero air (UZA) was systematically added to the instrument inlet tip to assess the contribution of background organic signal originating from the IVOC inlet or from within the instrument itself. In all cases, such signal was small compared to the overall background signal, indicating that any measurable IVOC background signal likely originates from surfaces within the exhaust and dilution tunnel. The background IVOC contribution to the total measured IVOCs was quantified through dynamic blank runs (sampling lab air through the engine manifold and dilution tunnel with the engine off). A total of two dynamic blanks were captured for each experiment: one prior to engine ignition ("pre-run") and another immediately following engine shutdown ("post-run"). Dynamic blanks were collected using the same sampling parameters (collection temperature, collection time, and system flows) used during engine-on exhaust IVOC measurements. The background temperature-dependent mass spectra acquired during the dynamic blank were subtracted from all engine-on IVOC measurements. For the results presented here, the "post-run" dynamic blank was subtracted from all engine-out IVOC emission measurements (see Figure S2 and discussion therein for additional details).

Instrument response was calibrated with syringe injections (10−600 nL min^{-1}; 250 μL syringe, Harvard Apparatus syringe pump) of eicosane ($C_{20}H_{42}$) into the inlet of the TD-EIMS.[28] This calibration approach ensures that the injected IVOCs are subject to identical sampling conditions as the engine exhaust IVOCs, thereby accounting for any potential losses within the IVOC inlet itself. Because all measurements are referenced to this one calibration compound, IVOC concentrations are given in "C_{20} equivalent" mass concentrations (μg C m^{-3}). Run-to-run variability in the TD-EIMS response reveals a calibration uncertainty of ±15%. This injection method was also used to introduce unburned fuel into the TD-EIMS to measure its mass spectrum. Given the configuration of the engine and dilution sampling system, losses upstream of the IVOC inlet (i.e., within the dilution or sampling tunnel) could not be characterized directly. If such losses were significant, the present measurements would represent lower limits to the IVOC emissions; however, by confining IVOC sampling intervals to steady-state temperature conditions, losses due to changing surface temperatures are likely to be minimal.

Emission Index. IVOC emissions are expressed in terms of an emission index (EI_{IVOC}), the mass of IVOCs emitted per kilogram of fuel consumed (mg kg^{-1}). Fuel consumption was not directly measured but rather was estimated from emitted CO_2 concentrations. EI_{IVOC} was calculated via eq 1:

$$EI_{IVOC} = (\Delta IVOC/\Delta CO_2)^*(T/P)^*4478 \quad (1)$$

where ΔIVOC is the background-subtracted mass concentration of IVOC (μg m^{-3}), ΔCO_2 is the background-subtracted CO_2 concentration (ppmv) measured at the IVOC sampling inlet (thereby taking dilution into account), T is the sampling temperature (K), and P is the ambient pressure (Torr). The

DOI: 10.1021/acs.est.5b03954
Environ. Sci. Technol. 2015, 49, 13483−13491

constant 4478 incorporates the CO_2 emission index of 3160 g CO_2 per kg fuel, which assumes 100% combustion efficiency of diesel fuel with a hydrogen-to-carbon ratio of 1.9.[28,31] This assumption of high combustion efficiency is likely valid because THC and CO constitute <0.5% of the total carbon emissions from this engine.

Δ Series Approach. The high-resolution mass spectra of the measured IVOCs are exceedingly complex. For ease of visualization and interpretation, mass spectra are described using the Δ series approach.[32] This approach combines ions with similar functionality but different number of CH_2 groups, with each Δ series grouping defined by $\Delta = m/z - 14n + 1$. Electron impact spectra are dominated by even-numbered Δ ions, most importantly the Δ = +2 series, associated with saturated hydrocarbons ($C_xH_{2x+1}^+$ ions from straight-chain and branched alkanes). Lower Δ values are associated with higher degrees of unsaturation in the parent organic molecule. Δ = 0 (C_xH_{2x-1}) ions are typically associated with branched alkanes and alkenes, Δ = −2 ions with cycloalkanes, Δ = −4 with bicycloalkanes, and Δ = −6 with tricycloalkanes. Similar approaches have been previously utilized for interpreting aerosol mass spectrometer data of particulate matter from chamber SOA[33] and in-use mobile combustion sources;[34,35] here, we extend its use for characterizing IVOC bulk composition.

Because of the dominance of hydrocarbon species in the engine exhaust, we categorize only the ions of formula $C_xH_y^+$ as Δ = +2, 0, −2, −4, and −6. Other ions are categorized as one of three additional groups: "aromatic", "oxidized", or "remainder". The "aromatic" grouping is defined as all ions with H/C ratios of ≤1.2 (which are not included in the Δ = +2 to −6 series), providing a rough metric of the contribution of aromatic ion fragments to the mass spectra. Likewise, the "oxidized" ion series includes all $C_xH_yO_z^+$ ions, providing information on the contribution of oxygenated organic species. The "remainder" series contains all other HR ions, which in this case are predominately odd Δ series ions. ^{13}C isotopes were not fit in the high resolution mass spectra and were therefore not included in analysis.

RESULTS AND DISCUSSION

Overview of Measurements. Operating parameters and emissions measurements from the cold-start/load-sweep experiment are shown in Figure 1. Engine operating parameters (speed, load, and exhaust gas temperatures) are provided in panels a and b, along with the CO_2 concentration measured at the IVOC inlet position. This concentration is used in the calculation of the emission index of the measured IVOCs (eq 1). The time series in Figure 1 begins with a cold-start ignition and a hold at engine idle (760 rpm, ∼ 0% load) to allow the engine manifold and exhaust sampling surfaces to reach thermal equilibrium. The engine load is then systematically increased, ramping through a series of low-, intermediate-, and high-load operating conditions, and is then stepped down across the same load points, returning the system to idle. This experimental design allows the semicontinuous measurements with the TD-EIMS (1 min of sampling every ∼8 min) to capture and characterize IVOC emissions for a range of engine operating conditions.

IVOC emissions were measured for two general types of operating conditions; transient and steady-state. Steady-state conditions refer to IVOC collection intervals during which engine and sampling system temperatures are constant. Transient operating conditions refer to IVOC collection intervals that coincide with a transition in engine operating state, which results in nonequilibrium temperature effects in the engine manifold and exhaust sampling system. During a transient state, the composition and magnitude of IVOC emissions may be influenced not only by the rapidly changing combustion conditions (equivalence ratio, temperature, pressure) but also by potential condensational or evaporative losses to/from the engine manifold and exhaust sampling surfaces. Here we operationally define steady-state conditions as collection intervals, during which the exhaust gas temperature is within ±10% of the average steady-state temperature for that load. For temperature ratios outside of this range, the collection interval is designated as a transient. During the load sweep, two transient states were sampled, shown as purple bars in Figure 1a. The first corresponds to the warm-up interval directly following engine ignition (cold-start transient), and the second refers to the engine acceleration from idle to 12% load. Steady-state and transient IVOC emission characteristics are described separately in the following sections.

The loading and fractional composition of the IVOC emissions are plotted in panels c and d of Figure 1. Each IVOC measurement is background-subtracted and integrated over the full desorption (i.e., with no volatility separation). Bulk IVOC composition is displayed in terms of contributions by each ion Δ series grouping, as described above. Despite changes to the IVOC emissions across the load sweep shown in Figure 1, we do not observe significant differences in the bulk IVOC volatility profile (Figure S3) as a function of engine load. This may indicate that different types of IVOCs emitted at different engine loads have similar volatility distributions. However, this is more likely a result of the dependence of desorption temperatures on IVOC concentrations. As engine load changes, this effect may shift the volatility measurement "window", possibly obscuring any changes to volatility distributions of the emissions. Thus, the role of engine load on IVOC volatility is difficult to assess in the present experiments, and so here we focus only the overall (volatility-averaged) IVOC emissions at each engine power.

Panels c and d of Figure 1 show that the magnitude and composition of the IVOC emissions are strongly dependent on engine load. Emissions are highest at engine idle; as engine load increases, total emissions decrease dramatically. Similarly, emissions at low engine powers are dominated by relatively saturated species (Δ = +2, 0, and −2), with the contributions of unsaturated species (lower Δ series ions and "aromatic" ions) increasing as engine load is increased. Figure 1 also reveals signs of a hysteresis effect on the magnitude of the IVOC emissions. As the engine load is decreased from 75% to idle, IVOC emissions are systematically lower (by up to a factor of 2) than they were during the increasing load ramp. This may be the result of improved combustion efficiency of the engine following the high temperatures and fuel flows necessary to reach and maintain the 75% load condition but could also reflect variable interactions (condensation and revolatilization) of IVOC emissions with the surfaces of the dilution tunnel itself. It is not possible to separate these two processes clearly; therefore, one or both processes may be impacting the measured IVOC emission profile throughout the load-sweep. We note that such potential interactions of IVOCs with surfaces is not unique to the present experiments and instead is likely to impact any emissions measurements in which dilution and sampling surfaces are not actively heated. The response of

DOI: 10.1021/acs.est.5b03954
Environ. Sci. Technol. 2015, 49, 13483−13491

measurements to preceding experimental conditions (engine operating parameters and/or surface temperatures) thus appears to play a role in recorded emission levels. Subtraction of the "post-run" dynamic blank (captured with a residually warm dilution-tunnel system), provides an initial correction for any IVOC signal originating from sampling surfaces. Given the near-real-time framework of the current experiment, it is also important to recognize that changes in IVOC concentration are assumed to be coincident (and instantaneous) with changes in CO_2 concentration.

Load-Dependent Steady-State IVOC Emission Indices. The load dependence of the IVOC emissions are shown in Figure 2. Given the IVOC hysteresis effect described above, we

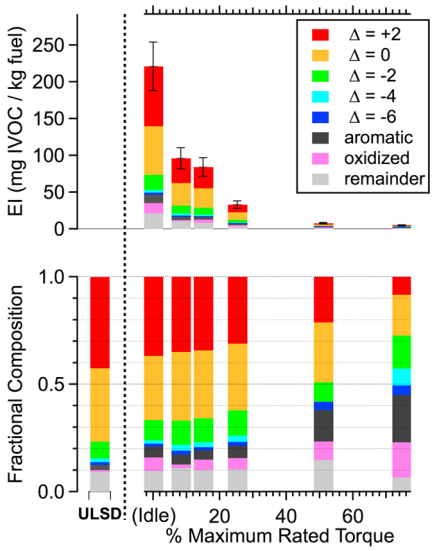

Figure 2. Steady-state composition and emission indices of IVOCs as a function of engine load. Upper panel: absolute emission indices. Lower panel: fractional composition of IVOC emissions, shown in terms of the Δ series of the mass spectrum (see text for details). For comparison, the fractional composition of unburned fuel is shown in the lower left. IVOC data for the 50% load condition were obtained from an additional load-sweep experiment, not shown in Figure 1. All data shown are averaged over the duty cycle of the TD-EIMS (1 min of collection every 8 min).

determine steady-state IVOC emissions factors by averaging the data from the upward and downward load sweeps together, presenting the averaged results as a function of engine load. This averaging serves to at least partially compensate for any dependence of measured IVOCs on the changing temperatures of the dilution tunnel surfaces, as described above; differences in the measurements at each load are small relative to changes in averaged emission factors over the load sweep. Results show that the average IVOC emission index decreases dramatically with increased engine loading from a maximum of 220 mg kg^{-1} at engine idle to only ~5 mg kg^{-1} at 75% load. This trend is consistent with differences in combustion efficiency at different engine loads. Because the engine is optimized for high-load conditions[27] and is least efficient at engine idle, IVOC emissions (at least those that are directly related to fuel combustion) are expected to decrease with increasing load. We have observed a similar relationship between IVOC emissions and engine load in our previous study of aircraft exhaust;[28] similar load-dependent trends in POA and THC emissions have also been observed from heavy-duty direct-injection diesel engines.[36]

The composition of the IVOCs also exhibits a major dependence on engine load. At low loads (≤25%), approximately 75−80% of IVOC ion signal is from Δ = +2, 0, and −2 ions, indicating the composition is dominated by alkanes, alkenes, and cycloalkanes. In fact, the Δ series composition of the engine-idle IVOC emissions bears close resemblance to that of unburned fuel (bottom left of Figure 2). This strongly suggests that under idle conditions, unburned fuel components may make up a large fraction of IVOC emissions, a result that is consistent with previous studies.[15,16] As load increases, the Δ = +2 contributions decrease from >40% of the total IVOC signal at idle to <10% of the signal at 75% power. The opposite trend is observed for ions corresponding to highly unsaturated species (Δ = −6 and aromatic ions), which together increase from ~5% at engine idle to more than 20% of the IVOC emissions at 75% load. Similarly, the fractional contribution of oxidized species to the total IVOC emissions is 6% at engine idle but is as high as 16% at 75% load. Somewhat smaller contributions from oxidized ions are observed at low-to-intermediate loads; the reason for this nonmonotonic behavior is not clear at present and highlights the need for further study of oxygenated IVOC emissions.

The Δ series approach used here suggests that at low engine loads, IVOC emissions are dominated by unburned fuel, with other IVOC sources becoming dominant at higher loads. This is illustrated in greater detail in Figure 3, which compares the relative intensities of the high-resolution ions for unburned ULSD fuel with exhaust IVOC at idle and at 75% load. The high-resolution mass spectra for exhaust at idle and ULSD fuel (Figure 3a) are highly correlated (R^2 = 0.94), with major ions (Δ = +2, 0, −2) falling on the 1:1 line, confirming the strong chemical similarity of these two mixtures. However, even at engine idle, some differences are clear. Oxidized ions, most notably with 3 or 5 carbon atoms ($C_5H_5O^+$, $C_5H_7O^+$, $C_5H_9O^+$, $C_3H_7O_3^+$, and $C_3H_9O_3^+$) are enhanced in engine-idle exhaust relative to the unburned fuel. Such oxygenated IVOCs could arise from the formation of long-chain (C_{10}-C_{20}) *n*-alkanoic acids[37] or ketone and aldehyde derivatives of poly aromatic hydrocarbons (oxy-PAH)[38,39] within the engine; however, additional speciated measurements are necessary for definitive source attribution. In addition, the engine-idle exhaust also exhibits elevated contributions from a few select "aromatic" ions, most importantly CH^+, C_6H^+, $C_6H_2^+$, and $C_7H_3^+$, indicating that the emissions are also enhanced in aromatic character relative to the unburned fuel.

In contrast to the engine-idle IVOC emissions, the composition of engine exhaust at 75% load is fundamentally different from unburned fuel (Figure 3b; R^2 = 0.34). Under this higher-load condition, the saturated aliphatic ions (Δ = +2 and Δ = 0) are depleted relative to the mass spectrum of the unburned fuel, and the strongly unsaturated ions (Δ = −4 and Δ = −6) are greatly enhanced. Most dramatic are the enhancements in aromatic and oxidized ions, indicating the increased formation of aromatic and oxygenated IVOCs at the higher temperatures and pressures of high-load engine operation. Figure S5 shows the relationship between the engine idle and 75% load IVOC mass spectra.

Figure 4 shows the contribution of unburned fuel to total IVOC emissions for all engine-load conditions studied, as estimated from spectral subtraction. In this approach, similar to that used previously for studying the oxidative aging of diesel

DOI: 10.1021/acs.est.5b03954
Environ. Sci. Technol. 2015, 49, 13483−13491

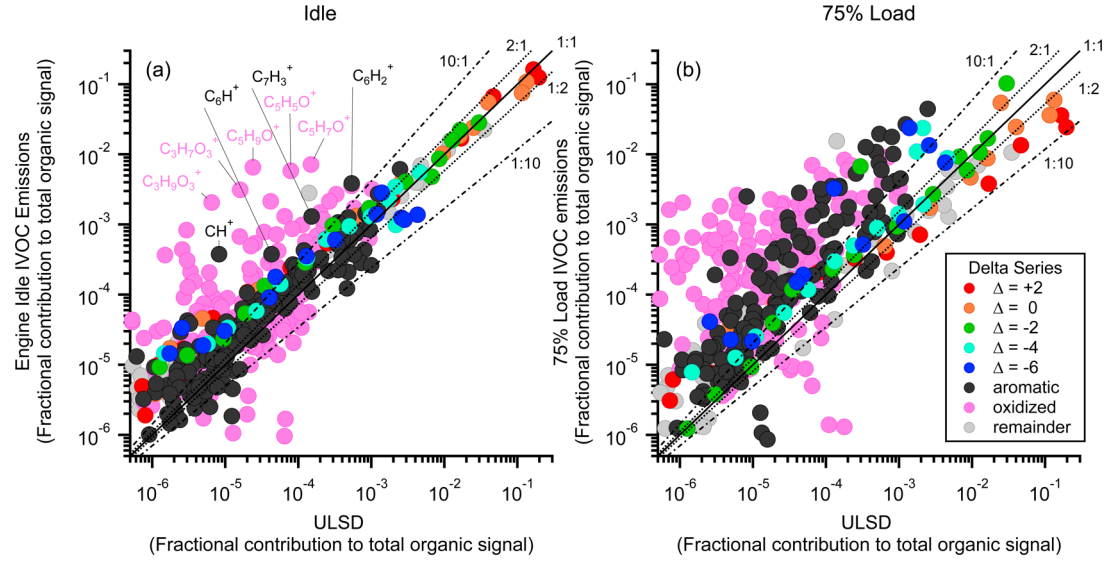

Figure 3. Mass-spectral comparison of fuel and IVOC exhaust measured at engine idle (panel a) and 75% load (panel b). Each ion is colored by its Δ series attribution. Unburned fuel IVOC spectra are plotted along the *x*-axis; deviations from the 1:1 line indicate chemical differences between emitted IVOCs and the pure fuel. Mass spectra from unburned fuel and engine idle exhaust IVOCs are chemically similar, while IVOC emissions at 75% power deviate substantially from the mass spectral composition of unburned fuel, with enhanced aromatic and oxidized ion signatures in the exhaust.

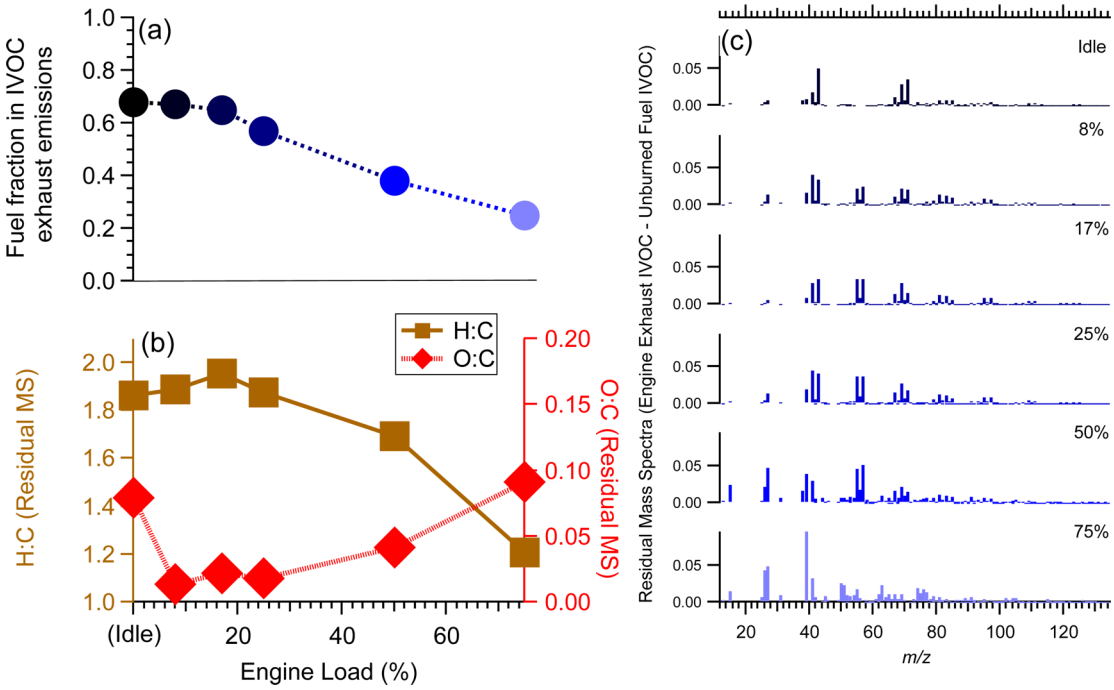

Figure 4. Contribution of unburned fuel to IVOC emissions and properties of remaining (nonfuel) emissions as a function of engine load, as determined from spectral subtraction; these fractions represent upper limits because other IVOC types may have similar mass spectra (see text). Panel a: fuel fraction in the IVOC exhaust as a function of engine load. Panels b and c: elemental abundance and residual mass spectra of nonfuel components for each load condition.

exhaust particles,[40] the unburned fuel mass spectrum is scaled by some factor and then subtracted from normalized exhaust IVOC mass spectra. The scaling factor is determined empirically at each load condition by finding the largest scaling factor possible for which no peaks in the subtracted mass spectrum are negative. This scaling factor is an upper limit to the fraction of engine exhaust derived from unburned fuel because other classes of organic species may have similar mass spectra. The residual (subtracted) spectra then provide a basis for assessing additional sources of IVOC (other than unburned fuel) that arise from the diesel combustion process.

As shown in Figure 4, at low (0−17%) engine loads, ∼ 65% of the IVOC ion signal is attributed to unburned fuel. The unburned fuel fraction then drops with increasing engine power and is only ∼25% of the IVOC emissions at 75% load. The elemental composition of the residual mass spectra show a coincident drop in the H:C ratio, from ∼1.9 at low loads to ∼1.2 at 75% load. This is consistent with the Δ series results

DOI: 10.1021/acs.est.5b03954
Environ. Sci. Technol. 2015, 49, 13483−13491

indicating the increasing importance of aromatic emissions with increasing load. The residual mass spectra (Figure 4c) show that low-load residual spectra retain many of the saturated ion signatures (Δ = +2, 0, −2). A possible source of these nonfuel aliphatic IVOC are *n*-alkyl fragments resulting from mild thermocracking (T = 250−400 °C) of lubricant molecules making up the dewaxed distillate.[41] At higher engine loads (50% and 75%) the composition of the residual spectra begins to shift toward lower Δ series ions with increasing degrees of unsaturation, as well as increasing levels of oxidation. This suggests the increasing importance of pyrolysis and partial oxidation of fuel and/or lubricant at these high engine loads.

Our load-dependent composition results (Figures 2−4) indicate that unburned fuel makes up the majority of IVOC emissions at low loads but also that nonfuel aliphatic and aromatic IVOC emissions, possibly arising from thermocracking, pyrolysis, or partial oxidation of fuel or lubricant molecules, also constitute an important fraction of the IVOC emission profile. To our knowledge, these represent the first measurements of the composition of diesel-exhaust IVOCs as a function of engine load. Nonetheless, these results are in qualitative agreement with previous IVOC composition measurements made over entire drive cycles. Schauer et al. measured IVOC emissions that were similar to IVOCs in pure diesel fuel[15] but with elevated levels of less-volatile PAHs and oxygenates (acids and carbonyls) in the exhaust. Similarly, Siegl et al. found evidence of enhancements in IVOC aromatics (such as 1,2-methylnapthalenes) in light duty diesel exhaust relative to unburned fuel.[16] The present measurements are also in agreement with our previous load-dependent measurements of aircraft exhaust,[28] which found that IVOC emissions at low loads were dominated by unburned fuel, whereas emissions at higher loads had increased aromatic and oxygenated character.

Transient Emissions. While the above discussion focuses on steady-state emissions, in which the engine manifold (and exhaust sampling surfaces) had reached near-thermal equilibrium with the exhaust gas, the time series of IVOC emission trends displayed in Figure 1 also includes one cold-start transient and one engine-load transient. The cold-start transient period is characterized by dramatic changes in the amount and chemical composition of IVOC emissions spanning the warm-up period. Immediately following engine ignition, the IVOC emission index is relatively small (∼28 mg kg^{-1}) and predominately composed of oxidized and aromatic ions. As the engine, exhaust lines, and emissions-sampling system gradually warm up (with dilute-exhaust temperatures rising from 25 to 42 °C), the IVOC emission index increases by nearly a factor of 10, reaching the steady-state IVOC emission index of ∼220 mg kg^{-1}. Over this ∼30 min interval, the composition of the emitted IVOCs evolves from highly unsaturated organic species to aliphatic species with a much higher degree of saturation (characterized by high intensities of Δ = +2, 0, and −2 ions, as in the steady-state idle emissions).

These results suggest that unheated engine-system and exhaust-sampling surfaces can greatly impact measured IVOC emission profiles, presumably due to condensational losses of IVOCs (particularly the aliphatic species). Cold-start emissions are generally thought to result in higher emissions due to the warm-up time associated with emission-control technologies.[42] However, for the untreated emissions sampled here, measured emissions are actually significantly lower because of losses to exhaust transfer lines, dilution tunnel surfaces, and sampling inlet walls. Such losses could lead to errors in IVOC measurements, especially when sampling and inlet surfaces are not actively heated. Understanding the influence of engine manifold and exhaust sampling surface temperatures is crucially important in IVOC emission-characterization studies, and experiments that neglect such considerations risk underestimating IVOC emission levels.

In contrast to the relatively gradual changes in IVOC emission index and composition observed during the cold-start transient, the engine load-transient (from idle to 12% load) is very short-lived. During this load-transient, the IVOC emission index was ∼300 mg kg^{-1}; this is substantially higher than the steady-state IVOC emission index at either idle or 12% load (220 and 95 mg kg^{-1}, respectively). The Δ series composition of the IVOCs measured during the idle-to-12% load transient is very similar to the composition of the steady-state engine idle IVOC composition, with spectral subtraction indicating an ∼70% contribution of unburned fuel to the measured IVOCs. This transient pulse of enhanced IVOC emissions may arise from the imperfect timing of fuel injection upon the initial increase in load demand on the idling engine. If this effect is routine during changes in engine load, low-load transients could be a major contributor to IVOC emissions.

Implications. Our results show that the amount and chemical composition of diesel engine IVOC emissions are highly dependent on engine load. The sources (unburned fuel or lubricant subjected to thermocracking, pyrolysis, and/or oxidation processes) and resultant impacts of the IVOC emissions likewise change with engine operation. Generally speaking, as engine load increases, IVOC emissions decrease dramatically (by almost 2 orders of magnitude going from engine idle to 75% load), and the chemical identity of the IVOCs themselves shift from saturated aliphatic species to more unsaturated and oxygenated species. The highest levels of emissions, from engine-idle and low-engine-load (≤25%) operation, arise mostly from unburned diesel fuel but also with significant contributions of nonfuel aliphatic species, which may result from mild thermocracking of lubricating oil constituents. The relative importance of lubricant-derived IVOC emissions appears to increase with increasing engine load. To understand the atmospheric implications of such load-dependent IVOC emissions, composition, and sources, the study of SOA formation from diesel emissions at a single operating state (most importantly engine power) would help connect individual IVOC formation processes within the engine to atmospheric PM formation. This work also demonstrates that continued SOA laboratory studies utilizing unburned (evaporated) diesel fuel could further inform the impact of engine-idle and low-load IVOC emissions, providing a means to assess how fuel reformulation may impact SOA formation and, hence, local and regional air quality.

The average steady-state engine idle IVOC emission index reported here is ∼220 mg kg^{-1}. The magnitude of idle IVOC emissions compares reasonably well with recent results from Gordon et al., who reported an unspeciated NMOG emission index of ∼140−160 mg kg^{-1} for the cold-start unified drive cycle (using a medium-duty diesel engine similar to the system used in this study). Neither engine system was equipped with emission control technology, so both studies provide information on the raw organic exhaust emissions. Despite source similarities, it remains difficult to directly compare the steady-state emissions reported here with the cumulative test-cycle-average emissions of Gordon et al., as the average emissions will tend to obscure the dramatic variability in IVOC

DOI: 10.1021/acs.est.5b03954
Environ. Sci. Technol. 2015, 49, 13483−13491

emissions that results from different engine loads. Gordon et al. also report that different drive-cycles result in significant changes in the emissions including a fivefold increase in HDDV NMOG emissions during a "creep and idle" cycle compared to a standard highway cycle, underscoring the disproportionate impact that low-load operating conditions can have on organic (IVOC) emissions. Similarly, Zhao et al., (2015) also found dramatically increased IVOC emissions under "creep-idle" conditions, with emissions relative to those under Unified Cycle conditions higher by a factor of 6× and 23× for non-ECT and ECT vehicles, respectively.[17] In the non-ECT case, the "creep and idle" cycle resulted in IVOC emission factors of ∼4000 mg kg^{-1} significantly higher than the IVOC emission factors reported here; however, this value was for an HDDV engine and so is not directly comparable with the present results Nevertheless, these results (from the present study, that of Gordon et al.,[18] and that of Zhao et al.[17] it is clear that emissions during engine idle and low-load operating states dominate the overall IVOC emissions from diesel combustion engines.

The focus of this study was on steady-state IVOC emissions, although two transients were captured. The two examples provide context for future experiments targeting transient IVOC emissions. Effects of load (most often via cold-start) transients are generally captured in drive-cycle tests, but devising and implementing transient-specific approaches to emissions-testing protocols will help quantify IVOC emission indices and more accurately assess the SOA formation potential of mobile sources. Such efforts would complement steady-state and cycle-average emissions characterization while also providing future targets for emission reductions.

■ ASSOCIATED CONTENT

Supporting Information

The Supporting Information is available free of charge on the ACS Publications website at DOI: 10.1021/acs.est.5b03954.

Cummins 2002 ISB 300 engine specifications, schematic of the engine exhaust sampling apparatus, summary of IVOC background subtraction, thermograms of the measured IVOC % series fractional composition, illustration of the day-to-day consistency in IVOC emissions characterization, and comparison of normalized IVOC mass spectra acquired during engine idle and 75% load operating conditions (PDF)

■ AUTHOR INFORMATION

Corresponding Author

*E-mail: escross@mit.edu.

Notes

The authors declare no competing financial interest.

■ ACKNOWLEDGMENTS

This work was supported by USEPA grant no. RD834560. Its contents are solely the responsibility of the grantee and do not necessarily represent the official views of the USEPA. Furthermore, USEPA does not endorse the purchase of any commercial products or services mentioned in the publication. E.S.C. was supported with a Camille and Henry Dreyfus Foundation environmental chemistry postdoctoral fellowship. Experiments were supported by the MIT Consortium to Optimize Lubricant and Diesel Engines for Robust Emission Aftertreatment Systems. Sponsorship from the following participants of the Consortium made this work possible: Caterpillar, Chevron/Oronite, Ciba Special Chemicals, Cummins, Detroit Diesel, Infineum, Komatsu, Lutek, NGK, Sud-Chemie, the U.S. Department of Energy Office of Energy Efficiency and Renewable Energy: Oak Ridge National Laboratory, and Valvoline. The authors thank Dr. Allen Robinson (CMU), Dr. John Storey (ORNL), and Drs. Andrew Lambe and Timothy Onasch (Aerodyne Research, Inc.) for helpful discussions.

■ REFERENCES

(1) Paulson, S. E. Neighborhood-scale air quality impacts of emissions from motor vehicles and aircraft. *Atmos. Environ.* **2013**, *80*, 310−321.

(2) Morawska, L.; Ristovski, Z.; Jayaratne, E. R.; Keogh, D. U.; Ling, X. Ambient nano and ultrafine particles from motor vehicle emissions: Characteristics, ambient processing and implications on human exposure. *Atmos. Environ.* **2008**, *42*, 8113−8138.

(3) Health Effects Institute.*Traffic-Related Air Pollution: A Critical Review of the Literature on Emissions, Exposure, and Health Effects*. Special Report 17; Health Effects Institute: Boston, 2010.

(4) Brunekreef, B.; Holgate, S. T. Air pollution and health. *Lancet* **2002**, *360*, 1233−1242.

(5) Pope, C. A., III; Dockery, D. W. Health Effects of Fine Particulate Air Pollution: Lines that Connect. *J. Air Waste Manage. Assoc.* **2006**, *56*, 709−742.

(6) May, A. A.; Nguyen, N. T.; Presto, A. A.; Gordon, T. D.; Lipsky, E. M.; Karve, M.; Gutierrez, A.; Robertson, W. H.; Zhang, M.; Brandow, C.; et al. Gas- and particle-phase primary emissions from in-use, on-road gasoline and diesel vehicles. *Atmos. Environ.* **2014**, *88*, 247−260.

(7) Hildemann, L. M.; Mazurek, M. A.; Cass, G. R.; Simoneit, B. R. Quantitative characterization of urban sources of organic aerosol by high-resolution gas chromatography. *Environ. Sci. Technol.* **1991**, *25*, 1311−1325.

(8) Rogge, W. F.; Hildemann, L. M.; Mazurek, M. A.; Cass, G. R.; Simoneit, B. R. Sources of fine organic aerosol. 2. Noncatalyst and catalyst-equipped automobiles and heavy-duty diesel trucks. *Environ. Sci. Technol.* **1993**, *27*, 636−651.

(9) Zhao, Y.; Hennigan, C. J.; May, A. A.; Tkacik, D. S.; de Gouw, J. A.; Gilman, J. B.; Kuster, W. C.; Borbon, A.; Robinson, A. L. Intermediate-Volatility Organic Compounds: A Large Source of Secondary Organic Aerosol. *Environ. Sci. Technol.* **2014**, *48*, 13743−13750.

(10) Jathar, S. H.; Miracolo, M. A.; Tkacik, D. S.; Donahue, N. M.; Adams, P. J.; Robinson, A. L. Secondary Organic Aerosol Formation from Photo-Oxidation of Unburned Fuel: Experimental Results and Implications for Aerosol Formation from Combustion Emissions. *Environ. Sci. Technol.* **2013**, *47*, 12886−12893.

(11) Robinson, A. L.; Donahue, N. M.; Shrivastava, M. K.; Weitkamp, E. A.; Sage, A. M.; Grieshop, A. P.; Lane, T. E.; Pierce, J. R.; Pandis, S. N. Rethinking organic aerosols: Semivolatile emissions and photochemical aging. *Science* **2007**, *315*, 1259−1262.

(12) Robinson, A. L.; Grieshop, A. P.; Donahue, N. M.; Hunt, S. W. Updating the Conceptual Model for Fine Particle Mass Emissions from Combustion Systems. *J. Air Waste Manage. Assoc.* **2010**, *60*, 1204−1222.

(13) Cheung, C. S.; Di, Y.; Huang, Z. *Atmos. Environ.* **2008**, *42*, 8843−8851.

(14) Wang, X.; Cheung, C. S.; Di, Y.; Huang, Z. Diesel engine gaseous and particle emissions fueled with diesel-oxygenate blends. *Fuel* **2012**, *94*, 317−323.

(15) Schauer, J. J.; Kleeman, M. J.; Cass, G. R.; Simoneit, B. R. T. Measurement of Emissions from Air Pollution Sources. 2. C_1 through C_{30} Organic Compounds from Medium Duty Diesel Trucks. *Environ. Sci. Technol.* **1999**, 33, 1578−1587.

DOI: 10.1021/acs.est.5b03954
Environ. Sci. Technol. 2015, 49, 13483−13491

(16) Siegl, W. O.; Hammerle, R. H.; Herrmann, H. M.; Wenclawiak, B. W.; Luers-Jongen, B. Organic emissions profile for a light-duty diesel vehicle. *Atmos. Environ.* **1999**, *33*, 797−805.
(17) Zhao, Y.; Nguyen, N. T.; Presto, A. A.; Hennigan, C. J.; May, A. A.; Robinson, A. L. Intermediate Volatility Organic Compound Emissions from On-Road Diesel Vehicles: Chemical Composition, Emission Factors, and Estimated Secondary Organic Aerosol Production. *Environ. Sci. Technol.* **2015**, DOI: *491151610.1021/acs.est.5b02841* (Article ASAP).
(18) Gordon, T. D.; Presto, A. A.; Nguyen, N. T.; Robertson, W. H.; Na, K.; Sahay, K. N.; Zhang, M.; Maddox, C.; Rieger, P.; Chattopadhyay, S.; et al. Secondary organic aerosol production from diesel vehicle exhaust: impact of aftertreatment, fuel chemistry and driving cycle. *Atmos. Chem. Phys.* **2014**, *14* (9), 4643−4659.
(19) ExxonMobile. The Outlook for Energy: A View to 2040. Technical repORT, Exxon Mobile Corporation, Irving, TX, 2014, 1−76.
(20) Bahreini, R.; Middlebrook, A. M.; de Gouw, J. A.; Warneke, C.; Trainer, M.; Brock, C. A.; Stark, H.; Brown, S. S.; Dube, W. P.; Gilman, J. B.; et al. Gasoline emissions dominate over diesel in formation of secondary organic aerosol mass. *Geophys. Res. Lett.* **2012**, *39*, L06805.
(21) Gentner, D. R.; Isaacman, G.; Worton, D. R.; Chan, A. W. H.; Dallmann, T. R.; Davis, L.; Liu, S.; Day, D. A.; Russell, L. M.; Wilson, K. R.; Weber, R.; Guha, A.; Harley, R. A.; Goldstein, A. H. Elucidating secondary organic aerosol from diesel and gasoline vehicles through detailed characterization of organic carbon emissions. *Proc. Natl. Acad. Sci. U. S. A.* **2012**, *109* (45), 18318−18323.
(22) Dunmore, R. E.; Hopkins, J. R.; Lidster, R. T.; Lee, J. D.; Evans, M. J.; Rickard, A. R.; Lewis, A. C.; Hamilton, J. F. Diesel-related hydrocarbons can dominate gas phase reactive carbon in megacities. *Atmos. Chem. Phys.* **2015**, *15*, 9983−9996.
(23) Ensberg, J. J.; Hayes, P. L.; Jimenez, J. L.; Gilman, J. B.; Kuster, W. C.; de Gouw, J. A.; Holloway, J. S.; Gordon, T. D.; Jathar, S.; Robinson, A. L.; et al. Emission factor ratios, SOA mass yields, and the impact of vehicular emissions on SOA formation. *Atmos. Chem. Phys.* **2014**, *14*, 2383−2397.
(24) Sappok, A. *Detailed Chemical and Physical Characterization of Ash Species in Diesel Exhaust Entering Aftertreatment Systems* **2007**, DOI: 10.4271/2007-01-0318.
(25) Sappok, A.; Wong, V. W. Lubricant-Derived Ash Properties and Their Effects on Diesel Particulate Filter Pressure-Drop Performance. *J. Eng. Gas Turbines Power* **2011**, *133*, 032805−12.
(26) Cross, E. S.; Sappok, A.; Fortner, E. C.; Hunter, J. F.; Jayne, J. T.; Brooks, W. A.; Onasch, T. B.; Wong, V. W.; Trimborn, A.; Worsnop, D. R.; Kroll, J. H. Real-Time Measurements of Engine-Out Trace Elements: Application of a Novel Soot Particle Aerosol Mass Spectrometer for Emissions Characterization. *J. Eng. Gas Turbines Power* **2012**, *134*, 072801−10.
(27) Sappok, A. Emissions and in-cylinder combustion characteristics of Fischer−Tropsch and conventional diesel fuels in a modern CI engine. Masters Thesis, Massachusetts Institute of Technology, Boston, MA, 2006.
(28) Cross, E. S.; Hunter, J. F.; Carrasquillo, A. J.; Franklin, J. P.; Herndon, S. C.; Jayne, J. T.; Worsnop, D. R.; Miake-Lye, R. C.; Kroll, J. H. Online measurements of the emissions of intermediate-volatility and semi-volatile organic compounds from aircraft. *Atmos. Chem. Phys.* **2013**, *13*, 7845−7858.
(29) Aiken, A. C.; DeCarlo, P. F.; Jimenez, J. L. Elemental Analysis of Organic Species with Electron Ionization High-Resolution Mass Spectrometry. *Anal. Chem.* **2007**, *79*, 8350−8358.
(30) Aiken, A. C.; DeCarlo, P. F.; Kroll, J. H.; Worsnop, D. R.; Huffman, J. A.; Docherty, K. S.; Ulbrich, I. M.; Mohr, C.; Kimmel, J. R.; Sueper, D.; et al. O/C and OM/OC Ratios of Primary, Secondary, and Ambient Organic Aerosols with High-Resolution Time-of-Flight Aerosol Mass Spectrometry. *Environ. Sci. Technol.* **2008**, *42*, 4478−4485.
(31) Herndon, S. C.; Rogers, T.; Dunlea, E. J.; Jayne, J. T.; Miake-Lye, R.; Knighton, B. Hydrocarbon Emissions from In-Use Commercial Aircraft during Airport Operations. *Environ. Sci. Technol.* **2006**, *40*, 4406−4413.
(32) McLafferty, F. W.; Turecek, F. *Interpretation of Mass Spectra*, 4th ed.; University Science Books: Mill Valley, CA, 1994.
(33) Bahreini, R.; Keywood, M. D.; Ng, N. L.; Varutbangkul, V.; Gao, S.; Flagan, R. C.; Seinfeld, J. H.; Worsnop, D. R.; Jimenez, J. L. Measurements of Secondary Organic Aerosol from Oxidation of Cycloalkenes, Terpenes, and m-Xylene Using an Aerodyne Aerosol Mass Spectrometer. *Environ. Sci. Technol.* **2005**, *39*, 5674−5688.
(34) Schneider, J.; Weimer, S.; Drewnick, F.; Borrmann, S.; Helas, G.; Gwaze, P.; Schmid, O.; Andreae, M. O.; Kirchner, U. Mass spectrometric analysis and aerodynamic properties of various types of combustion-related aerosol particles. *Int. J. Mass Spectrom.* **2006**, *258*, 37−49.
(35) Canagaratna, M. R.; Jayne, J. T.; Ghertner, D. A.; Herndon, S.; Shi, Q.; Jimenez, J. L.; Silva, P. J.; Williams, P.; Lanni, T.; Drewnick, F.; Demerjian, K. L.; Kolb, C. E.; Worsnop, D. R. Chase Studies of Particulate Emissions from in-use New York City Vehicles. *Aerosol Sci. Technol.* **2004**, *38*, 555−573.
(36) Kweon, C.-B.; Okada, S.; Foster, D. E.; Bae, M.-S.; Schauer, J. J. *Effect of engine operating conditions on particle-phase organic compounds in engine exhaust of a heavy-duty direct-injection (DI) diesel engine* **2003**, DOI: 10.4271/2003-01-0342.
(37) Simoneit, B. Characterization of Organic Constituents in Aerosols in Relation to Their Origin and Transport: A Review. *Int. J. Environ. Anal. Chem.* **1986**, *23*, 207−237.
(38) Rogge, W. F.; Mazurek, M. A.; Hildemann, L. M.; Cass, G. R.; Simoneit, B. Quantification of Urban Organic Aerosols at a Molecular-Level - Identification, Abundance and Seasonal-Variation. *Atmos. Environ., Part A* **1993**, *27*, 1309−1330.
(39) Jensen, T. E.; Hites, R. A. Aromatic diesel emissions as a function of engine conditions. *Anal. Chem.* **1983**, *55*, 594−599.
(40) Kroll, J. H.; Smith, J. D.; Worsnop, D. R.; Wilson, K. R. Characterisation of lightly oxidised organic aerosol formed from the photochemical aging of diesel exhaust particles. *Environmental Chemistry* **2012**, *9*, 211−220.
(41) Kissin, Y. V. Acyclic components in dewaxed heavy distillates. *Fuel* **1990**, *69*, 1283−1291.
(42) George, I. J.; Hays, M. D.; Snow, R.; Faircloth, J.; George, B. J.; Long, T.; Baldauf, R. W. Cold Temperature and Biodiesel Fuel Effects on Speciated Emissions of Volatile Organic Compounds from Diesel Trucks. *Environ. Sci. Technol.* **2014**, *48*, 14782−14789.

DOI: 10.1021/acs.est.5b03954
Environ. Sci. Technol. 2015, 49, 13483−13491